



# Study on the application mechanism and mechanics of steel slag in composite cementitious materials

Zhimin Chen<sup>1</sup> · Kun Tu<sup>1</sup> · Rui Li<sup>1</sup> · Jiaxiang Liu<sup>1</sup> Received: 11 July 2020 / Accepted: 7 October 2020 / Published online: 16 October 2020  
© Springer Nature Switzerland AG 2020

## Abstract

Enormous demand and production for cement and concrete lead to a sharp increase in carbon dioxide emissions, and alternatives to cement are urgently needed to produce green cement and concrete. This paper is aimed at exploring the feasibility of using steel slag (SS) and granulated blast furnace slag (GBFS) to prepare cementitious materials. Mineral phases of SS are determined and observed by X-ray diffraction and backscattered electron microscopy. By measuring the compressive strength of mortar samples, the composite effect of SS-GBFS is analyzed and compared. Results show that SS can replace cement by 10%–30%, and the long-term strength of the prepared binary cementitious material is higher than that of cement. SS and GBFS can replace up to 50% of the cement. The strength of SS-GBFA-C ternary cementitious material is higher than that of SS-C, SS and GBFS promote mutually in cementitious materials.

**Keywords** Steel slag · Granulated blast furnace slag · Compressive strength · Supplementary cementitious material

## 1 Introduction

Portland cement production is an energy-intensive consumption process, and the cement industry accounts for 5%–8% of global carbon dioxide emissions annually [1–4]. The rapid development of China's construction, road and bridge construction industry leads to a great demand for concrete and cement. China's cement yield has been ranked first in the world for exceeding 20 years [5]; engineers and scientists have been searching for secondary raw materials that could substitute cement and advance the properties of cement. On the one hand, to reduce depletion of raw materials for cement production is of major importance for the prospect of developing sustainable construction materials and conserving natural resources. On the other hand, reducing the consumptions of heat and electricity to obtain these materials could indirectly curtail carbon dioxide emissions [6].

In recent years, cement and concrete composites have developed rapidly; cement mixtures containing different kinds of supplementary cementitious materials (SCMs) effectually reduce the dosage of cement powder. As stated by [7–10], SCMs can be categorized into industrial wastes, such as fly ash, silica fume, ground granulated blast furnace slag, agriculture wastes and aquaculture wastes. The application of SCMs in practical building materials shrinks the use of cement and reduces the emission of carbon dioxide.

Steel slag (SS) and granulated blast furnace slag (GBFS) are by-products of the production process of iron and steel industry, accounting for 30% of the total industrial by-products in China [11]. The chemical and mineral compositions of SS and GBFS are approximating to cement, and researches indicated that SS and GBFS could be used as aggregates, SCMs and binder in the cement and concrete industry [1]. GBFS has been widely used in cement and concrete as SCMs. Nevertheless, the effective utilization

✉ Jiaxiang Liu, ljxpost@263.net | <sup>1</sup>Beijing Key Laboratory of Electrochemical Process and Technology for Materials, Beijing University of Chemical Technology, Beijing 100029, China.



rate of SS is low, only about 22%, because of its low hydration property and poor soundness [12]. The output of SS accounts for 15–20% by mass of the total output of crude steel [13]. The accumulation of SS not only is a waste of resources, but also pollute to the environment [14, 15].

Reddy et al. [16] detected that the strength of water-quenched SS as hydraulic cementitious materials is up to 42.7 MPa after 28 days. Papayianni and Anastasiou [17] studied the replacement of cement with 30% SS and 50% FA as cementitious materials, and the concrete made by replacing some coarse aggregate with SS has higher compressive strength (> 70 MPa), higher abrasion resistance and fracture toughness than ordinary cement concrete. Sheen et al. [18] studied the properties of green concrete obtained by replacing coarse aggregate and fine aggregate with SS; results show that the compressive strength of concrete made from 100% SS replacing fine aggregate is higher than that of ordinary concrete.

The wide application and short supply of GBFS have brought new challenges to the cement industry. On the contrary, the low utilization rate of SS has not been solved so far. In order to improve the utilization of SS and reduce the load on the cement industry, this paper aimed at mixing GBFS and SS to cement, preparing composite cementitious materials. The interaction among SS, GBFS and cement was studied by characterizing the hydration properties of the material. At the same time, the effect of raw material ratio on the mechanical properties of composite cementitious materials is explored to determine the optimal mixing ratio between SS and GBFS in cement.

## 2 Materials and methods

### 2.1 Materials

SS produced by Xinyu Iron And Steel Co. Ltd obtained by crushing, removing iron, grinding and sifting has a density of 3.91 g/cm<sup>3</sup> and a specific surface area of 469 m<sup>2</sup>/kg. Industrial-grade GBFS powder is of a density of 2.90 g/cm<sup>3</sup> and a specific surface area of 354 m<sup>2</sup>/kg. Tap water and ISO standard sand were used to prepare mortar. Table 1 shows the main chemical composition of C (cement), SS and GBFS in this research.

**Table 1** Chemical composition of raw materials

Raw materials	Mass percentage (%)									
	SiO <sub>2</sub>	Al <sub>2</sub> O <sub>3</sub>	Fe <sub>2</sub> O <sub>3</sub>	CaO	MgO	FeO	Na <sub>2</sub> O	SO <sub>3</sub>	f-CaO	LOI
C	21.78	5.17	0.49	65.21	4.43	–	0.13	2.79	0.86	1.33
SS	12.86	1.70	13.09	54.64	8.36	9.35	–	–	2.39	1.71
GBFS	31.98	16.74	0.75	38.49	10.11	–	–	1.93	0.43	0.22

## 2.2 Methods

### 2.2.1 Determination and observation of mineral phases

X-ray diffraction was used to determine the chemical and mineral compositions of SS. Mineral phases of SS were observed and identified by backscattered electron (BSE) imaging technique and the element content of the surface microregion was analyzed by energy-dispersive X-ray spectroscopy (EDX). The surface morphology of SS–C after hydration was analyzed by scanning electron microscope (SEM). TG was used to analyze the hydration mechanism of composite cementitious materials.

### 2.2.2 Strength test of mortar specimens

The proportion of SS and GBFS mixed with cement is shown in Table 2. Mortar specimens were prepared in the 40 mm × 40 mm × 160 mm mold. After molding, put into standard constant temperature and humidity curing box (YH-40B) for 24 h and then demold, curing at BWJ–1 automatic cement curing water tank. Curing time was from the time of specimen molding to the time of testing the flexural and compressive strength, which was 3d, 7d and 28d, respectively, and the time error was less than 1 h. During the experiment, the temperature was controlled at 20 °C ± 1 °C, the relative humidity was more than 50%, and the humidity of standard curing box was more than 90%.

## 3 Results and discussion

### 3.1 Mineral phase in SS

Figure 1 shows the X-ray diffraction pattern of SS powder. The results show that the minerals in SS mainly included tricalcium silicate (C<sub>3</sub>S), ferroaluminum–calcium phase (Ca<sub>2</sub>[Fe, Al]<sub>2</sub>O<sub>5</sub>), calcium carbonate (CaCO<sub>3</sub>), RO phase (MgO, FeO and MnO solid solution), free calcium oxide (f-CaO), calcium hydroxide (CH) and dicalcium silicate (C<sub>2</sub>S). C<sub>3</sub>S and C<sub>2</sub>S in SS were the main sources of cementitious properties. However, C<sub>3</sub>S and C<sub>2</sub>S in SS are formed by melting at 1650 °C at high temperature, resulting in

**Table 2** Proportion of mortar samples

Samples	Cement/%	SS/%	GBFS/%	Samples	Cement/%	SS/%	GBFS/%
S0	100	0	–	S40G10	50	40	10
S10	90	10	–	S35G15	50	35	15
S20	80	20	–	S30G20	50	30	20
S30	70	30	–	S25G25	50	25	25
S40	60	40	–	S20G30	50	20	30
S50	50	50	–	S48G12	40	48	12
S60	40	60	–	S42G18	40	42	18
S32G8	60	32	8	S36G24	40	36	24
S28G12	60	28	12	S30G30	40	30	30
S24G16	60	24	16	S24G36	40	24	36
S20G20	60	20	20				
S16G24	60	16	24				

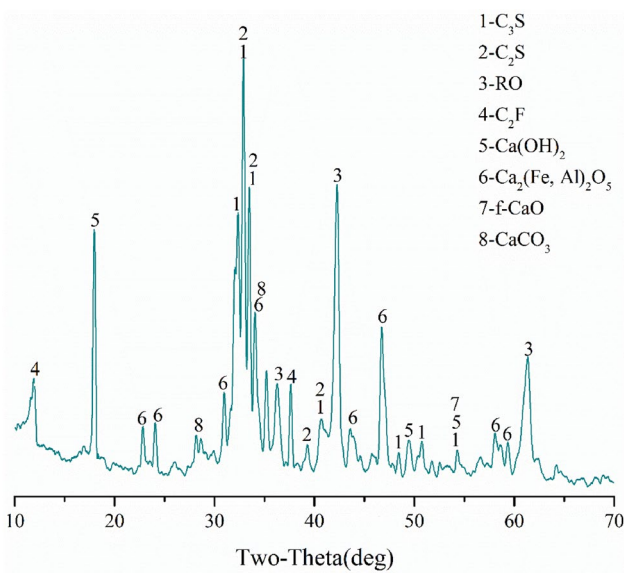


**Fig. 1** X-ray diffraction pattern of SS

many vitreous bodies, relatively dense structure and low cementitious activity [19].

Figure 2 presents the BSE images of steel slag, and the EDX analysis results are listed in Table 3. The minerals in SS

were mainly silicate including  $C_3S$  and  $C_2S$ , RO phase, ferroaluminum–calcium phase and free calcium oxide, which was basically consistent with X-ray diffraction analysis as shown in Fig. 1. RO phase was generally considered to have no hydration activity [5], but accounts for 20–30% in SS, resulting in lower relative content of cementitious active substances in SS than GBFS and cement. F–CaO is the main factor leading to poor volume stability of SS [20, 21].

### 3.2 Binary cementitious material

#### 3.2.1 Strength analyses

Figure 3 shows the compressive strength of SS-C cementitious material with different SS contents. The early strength (3d) of the mortar sample prepared by SS instead of part of cement was lower than that of pure cement. With the increase in the SS content, the early strength of the composite cementitious material decreased gradually, and the strength of the medium (7d) and long-term (28d) increased first and then decreased. The binary cementitious material with 10% SS content has the best mechanical properties, and the compressive strength of 7d and 28d is higher than that of pure cement. The change of the

**Fig. 2** BSE images of various mineral phases in SS

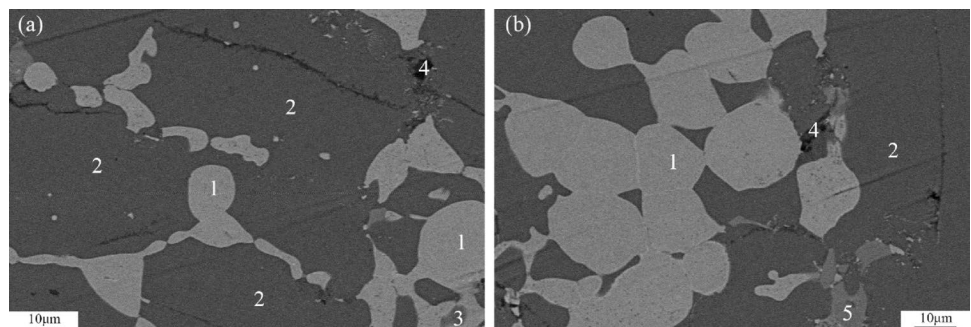
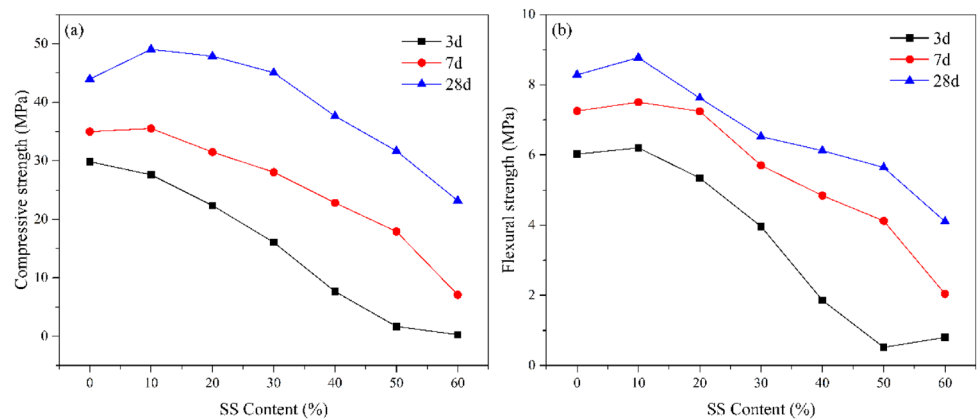


**Table 3** EDX analysis results of various mineral phases in SS

Selected areas	Atomic percentage (%)						
	O	Mg	Al	Ca	Si	Mn	Fe
1	54.89	17.01	–	0.27	–	3.41	24.43
2	62.36	0.48	–	24.57	12.42	–	0.26
3	59.44	4.46	–	16.83	10.06	1.14	8.08
4	60.13	1.56	5.21	9.58	4.76	0.68	5.26
5	67.02	0.43	4.40	20.88	2.89	–	4.38

**Fig. 3** Compressive strength (a) and flexural strength (b) of SS-C binary composites



flexural strength of SS-C cementitious material has a similar pattern.

When the content of SS was higher than 30%, the compressive strength of the sample decreased obviously, which limits the use of SS in large quantities.

### 3.2.2 Activity index

Figure 4 presents the activity index of 7d and 28d of the mortar samples with different SS contents. The activity index of SS-C binary composites decreased with the addition of SS. When SS was added with no more than 30%, the activity index of SS-C composite powder for 7d was above 80%, and that for 28d was above 100%. The high activity index of composite cementitious materials in the early hydration age benefited from the filler effect of SS in cement.

### 3.3 Ternary cementitious material

Figure 5 shows the compressive strength of ternary cementitious material. As the cement content decreased, the compressive strength of the samples decreased significantly. When the amount of cement was constant, the strength of cementitious materials increased with the increase in the GBFS content. SS and GBFS can replace 50% cement at most. When cement content in ternary cementitious material was 40%, the strength of the paste was lower than that of cement. By comparing the compressive

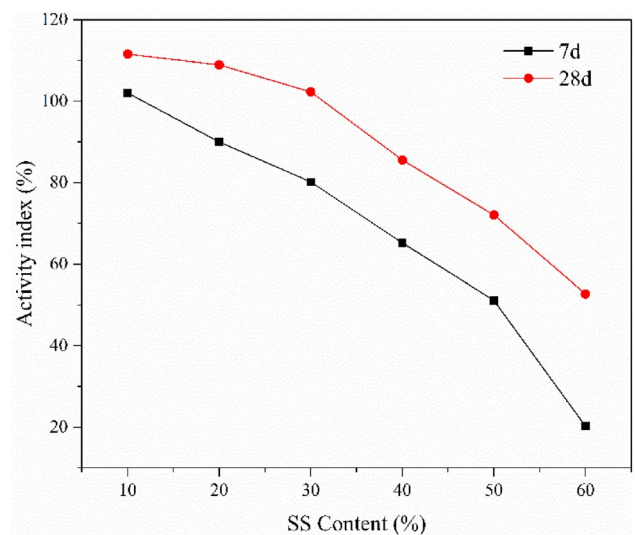


**Fig. 4** Activity index of SS-C binary composites cementitious materials

strength of cement, the 28d compressive strength of composite cementitious material was in the order of S16G24 > S20G20 > S10 > S20 > S20G30 > S25G25 > S24G16 > S30 > C. The flexural strength of SS-GBFS-C cementitious material has a similar pattern, but the 28d flexural strength of S24G16 was higher than other samples.

Among cement-based cementitious materials, SS accounts for 16% and GBFS accounts for 24%, the 28d



**Fig. 5** Compressive strength (a) and flexural strength (b) of SS-GBFS-C ternary cementitious materials

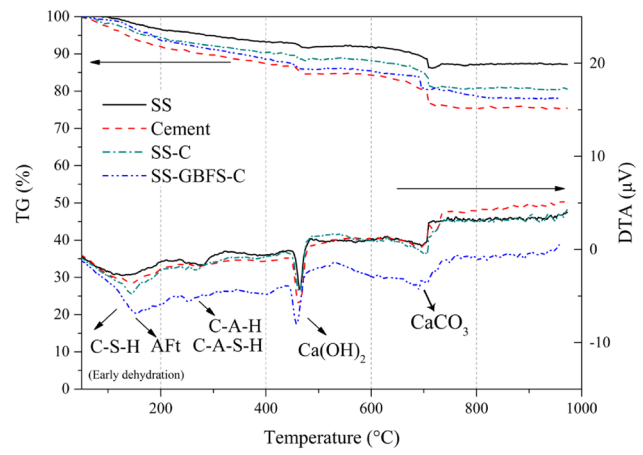
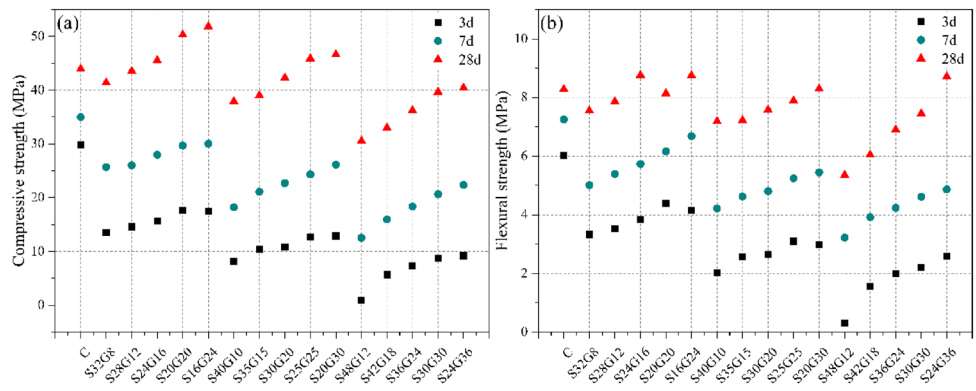


**Fig. 6** TG-DTA pattern of binary and ternary cementitious materials

compressive strength of the paste reached 51.85 MPa, and its mechanical properties were far superior to pure cement (43.95 MPa). Meanwhile, the mechanical properties of ternary composite cementitious materials were generally better than that of binary composite cementitious materials, which indicated that the strength enhancement of mixing SS and GBFS was obviously stronger than that of single-doped SS.

**3.4 Thermogravimetric analysis**

Figure 6 shows the TG-DTA curve of SS-C (S50) and SS-GBFS-C (S25G25) hardened slurry hydrated for 28 days. SS-C and SS-GBFS-C hardened slurry has three obvious endothermic peak between 50 °C and 1000 °C as presented in DTA curve: early dehydration endothermic peak of C-S-H and AFt between 100 and 200 °C, dehydration endothermic peak of CH between 440 and 475 °C, and decarbonation endothermic peak between 600 and 750 °C.

After 28 days of hydration, the CH content of binary cementitious and ternary cementitious calculated by mass loss was 12.99%–9.29%, respectively.

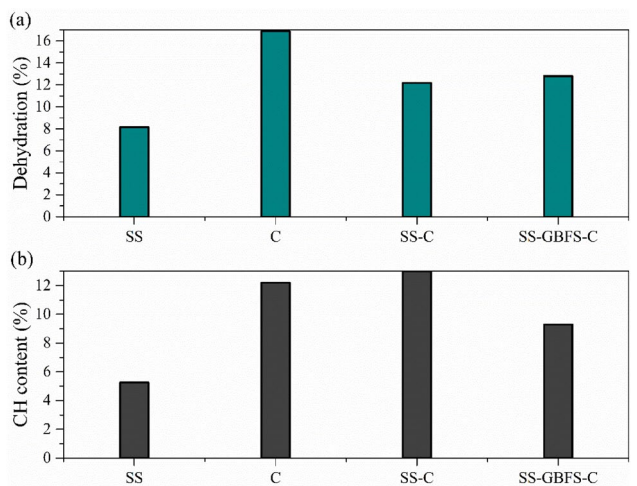


**Fig. 7** Dehydration bound water content of binary and ternary cementitious materials. Content of binary and ternary cementitious materials. a Amount of dehydration of C-S-H and AFt, b CH content

**3.5 The interaction of SS and GBFS in cementitious materials**

Figure 7 presents the amount of dehydration of the hydration products C-S-H and AFt (Fig. 7a) and the CH content in the cementitious material after hydration (Fig. 7b). The total dehydration of CSH and AFt in the ternary cementitious material after hydration is higher than that of the binary cementitious material, but the overall dehydration was lower than that of pure cement.

The binary cementitious materials will produce more CH after hydration, while ternary cementitious materials consume CH due to the pozzolanic reaction of GBFS, resulting in lower CH content after hydration than binary cementitious materials and lower than pure cement.

GBFS has hydration activities and pozzolanic activities, which means that the CH was consumed and C-S-H gels were produced during its reaction process [22, 23]. Therefore, in ternary cementitious materials, the CH

produced by the hydration of SS can be provided for GBFS consumption, which participates in the pozzolanic reaction of GBFS and promotes the hydration reaction of SS. The ternary cementitious material has high strength, more dehydration of the hydration products CSH and AFt, and low content of the hydration product CH, which confirms the mutual promotion between GBFS and SS.

## 4 Conclusion

GBFS is widely used as cementitious materials to replace cement. However, the application of SS is restricted by its content in cement. In this paper, SS and GBFS were used as supplementary cementitious materials to mix cement to prepare binary and ternary cementitious materials. The main conclusions are as follows:

- (1) The mineral phases in SS mainly contain  $C_2S$ ,  $C_3S$ , RO phase,  $C_2F$ ,  $Ca_2(Fe, Al)_2O_5$ ,  $f-CaO$  and so on. The main cementitious active substances and hydration products of SS are similar to cement.
- (2) The mechanical properties of binary cementitious prepared by SS instead of cement are better than cement, but the compressive strength of binary cementitious material with SS content over 30% decreases obviously. SS and GBFS can replace up to 50% cement, and by changing the proportion of SS and GBFS, the mechanical properties of the prepared ternary cementitious material are obviously better than cement.
- (3) In the hydration process of binary and ternary cementitious materials, SS can produce  $Ca(OH)_2$  and C-S-H gel, and the pozzolanic reaction of GBFS can consume  $Ca(OH)_2$  to produce more C-S-H gel. When SS and GBFS are applied together with cement-based cementitious material, they can promote each other and accelerate hydration reaction and pozzolanic reaction.

**Acknowledgements** This work was supported by the National Natural Science Foundation of China (Grant No. 51874013).

## Compliance with ethical standards

**Conflict of interest** The authors declare that we have no conflict of interest.

**Data availability statement** All data, models or code generated or used during the study are available in a repository online in accordance with funder data retention policies.

## References

1. Mo L, Zhang F, Deng M, Jin F, Altabbaa A, Wang A (2017) Accelerated carbonation and performance of concrete made with steel slag as binding materials and aggregates. *Cem Concr Compos* 83:138–145. <https://doi.org/10.1016/j.cemconcomp.2017.07.018>
2. Scrivener KL, Kirkpatrick RJ (2008) Innovation in use and research on cementitious material. *Cem Concr Res* 38(2):128–136. <https://doi.org/10.1016/j.cemconres.2007.09.025>
3. Turner LK, Collins FG (2013) Carbon dioxide equivalent (CO<sub>2</sub>e) emissions: a comparison between geopolymer and OPC cement concrete. *Constr Build Mater* 43:125–130. <https://doi.org/10.1016/j.conbuildmat.2013.01.023>
4. Wang Y, He X, Su Y, Tan H, Yang J, Lan M et al (2018) Self-hydration characteristics of ground granulated blast-furnace slag (GGBFS) by wet-grinding treatment. *Constr Build Mater* 167:96–105. <https://doi.org/10.1016/j.conbuildmat.2018.01.178>
5. Wang Q, Yan P, Feng J (2011) A discussion on improving hydration activity of steel slag by altering its mineral compositions. *J Hazard Mater* 186(2–3):1070–1075. <https://doi.org/10.1016/j.jhazmat.2010.11.109>
6. Yanfeng L (2009) Recycling of steel slag for energy saving and its application in high performance concrete. *Asia-Pacific Power Energy Eng Conf IEEE*. <https://doi.org/10.1109/APPEEC.2009.4918641>
7. Lothenbach B, Scrivener K, Hooton RD (2011) Supplementary cementitious materials. *Cem Concr Res* 41(12):1244–1256. <https://doi.org/10.1016/j.cemconres.2010.12.001>
8. Aprianti S, Evi. (2016) A huge number of artificial waste material can be supplementary cementitious material (SCM) for concrete production—a review part ii. *J Clean Prod* 142(4):4178–4194. <https://doi.org/10.1016/j.jclepro.2015.12.115>
9. Paris JM, Roessler JG, Ferraro CC, Deford HD, Townsend TG (2016) A review of waste products utilized as supplements to Portland cement in concrete. *J Clean Prod* 121:1–18. <https://doi.org/10.1016/j.jclepro.2016.02.013>
10. Mo KH, Johnson Alengaram U, Jumaat MZ, Yap SP, Lee SC (2016) Green concrete partially comprised of farming waste residues: a review. *J Clean Prod* 117:122–138. <https://doi.org/10.1016/j.jclepro.2016.01.022>
11. Guo X, Shi H (2013) Modification of steel slag powder by mineral admixture and chemical activators to utilize in cement-based materials. *Mater Struct* 46(8):1265–1273. <https://doi.org/10.1617/s11527-012-9970-7>
12. Wang Q (2012) Influence of initial alkalinity on the hydration of steel slag. *Sci China Technol Sci* 55(12):3378–3387. <https://doi.org/10.1007/s11431-012-4830-9>
13. Han F, Zhang Z, Wang D, Yan P (2015) Hydration heat evolution and kinetics of blended cement containing steel slag at different temperatures. *Thermochim Acta* 605:43–51. <https://doi.org/10.1016/j.tca.2015.02.018>
14. Yüksel İ (2018) A review of steel slag usage in construction industry for sustainable development. *Environ Dev Sustain* 19(2):1–16. <https://doi.org/10.1007/s10668-016-9759-x>
15. Li Y, Liu Y, Gong X, Nie Z, Cui S, Wang Z et al (2015) Environmental impact analysis of blast furnace slag applied to ordinary Portland cement production. *J Clean Prod* 120:221–230. <https://doi.org/10.1016/j.jclepro.2015.12.071>
16. Reddy AS, Pradhan RK, Chandra S (2006) Utilization of basic oxygen furnace (BOF) slag in the production of a hydraulic cement binder. *Int J Miner Process* 79(2):98–105. <https://doi.org/10.1016/j.minpro.2006.01.001>
17. Papayianni I, Anastasiou E (2010) Production of high-strength concrete using high volume of industrial by-products. *Constr*

- Build Mater 24(8):1412–1417. <https://doi.org/10.1016/j.conbuildmat.2010.01.016>
18. Sheen YN, Wang HY, Sun TH (2014) Properties of green concrete containing stainless steel oxidizing slag resource materials. *Constr Build Mater* 50:22–27. <https://doi.org/10.1016/j.conbuildmat.2013.09.017>
  19. Zhang T, Yu Q, Wei J, Li J, Zhang P (2011) Preparation of high performance blended cements and reclamation of iron concentrate from basic oxygen furnace steel slag. *Resour Conserv Recycl* 56(1):48–55. <https://doi.org/10.1016/j.resconrec.2011.09.003>
  20. Jia R, Liu J, Jia R (2017) A study of factors that influence the hydration activity of mono-component cao and bi-component CaO/Ca<sub>2</sub>Fe<sub>2</sub>O<sub>5</sub> systems. *Cem Concr Res* 91:123–132. <https://doi.org/10.1016/j.cemconres.2016.11.011>
  21. Liu J, Guo RH (2018) Applications of steel slag powder and steel slag aggregate in ultra-high performance concrete. *Adv Civ Eng*. <https://doi.org/10.1155/2018/1426037>
  22. Wang YB, He XY, Su Y, Yang J, Strnadel B, Wang XJ (2019) Efficiency of wet-grinding on the mechano-chemical activation of granulated blast furnace slag (GBFS). *Constr Build Mater* 199:185–193. <https://doi.org/10.1016/j.conbuildmat.2018.11.245>
  23. Mohan A, Mini KM (2018) Strength and durability studies of SCC incorporating silica fume and ultra fine GGBS. *Constr Build Mater* 171:919–928. <https://doi.org/10.1016/j.conbuildmat.2018.03.186>

**Publisher's Note** Springer Nature remains neutral with regard to jurisdictional claims in published maps and institutional affiliations.